Carbohydrate Polymers 92 (2013) 1402–1407

Contents lists available at SciVerse ScienceDirect

Carbohydrate Polymers

journal homepage: www.elsevier.com/locate/carbpol

Stabilisation of silver and copper nanoparticles in a chemically modified chitosan matrix

Anand D. Tiwari, Ajay K. Mishra*, Shivani B. Mishra, Alex T. Kuvarega, Bhekie B. Mamba

Department of Applied Chemistry, University of Johannesburg, P.O. Box 17011, Doornfontein 2028, South Africa

ARTICLE INFO

Article history:
Received 3 August 2012
Received in revised form 3 October 2012
Accepted 4 October 2012
Available online 12 October 2012

Keywords:
Stabilisation
Silver
Copper
Nanoparticle
Chitosan
Optical property

ABSTRACT

This work describes the stabilisation of silver and copper nanoparticles in chemically modified chitosan colloidal solution. Chitosan-N-2-methylidene-hydroxy-pyridine-6-methylidene hydroxy thiocarbohydrazide (CSPTH) was used as a stabilising and reducing agent for silver and copper nanoparticles. The modified chitosan derivatives and the synthesised nanoparticles were characterised by Fourier transform infrared (FT-IR) spectroscopy, Ultraviolet–visible (UV–Vis) spectroscopy and X-ray diffraction (XRD). Particle size, morphology and segregation of the nanoparticles were determined by transmission electron microscopy (TEM). The size of the nanoparticles was found to be less than 20 nm and 50 nm for silver and copper nanoparticles, respectively. These nanoparticles were stabilised in a chemically modified chitosan solution and their properties were studied using fluorescence spectroscopy, photoluminescence spectroscopy and surface-enhanced Raman scattering (SERS). The optical properties of silver nanoparticles in surface plasmon band (SPB) were enhanced at 407 nm compared to those of copper nanoparticles. Fluorescence (400 nm and 756 nm), photoluminescence (450 and 504 nm) and Raman scattering (1382 and 1581 cm^{-1}) properties for the copper nanoparticles were superior to those of the silver nanoparticles.

1. Introduction

The synthesis of metal nanoparticles is a subject of current interest due to their unique properties and promising applications (Cobley, Rycenga, Zhou, Li, & Xia, 2009; Li, Camargo, Lu, & Xia, 2009; Sharma et al., 2009; Sun & Xia, 2002; Yavuz et al., 2009). The synthetic procedure for fabricating metal nanoparticles can be divided into two stages: the reduction of metal salts and the capping by a protective agent. Capping prevents the nanoparticles from aggregation thus allowing segregation of the metal nanoparticles (Quiros et al., 2002). Among the many metal nanoparticles, silver nanoparticles (AgNPs) have received considerable attention due to their attractive physico-chemical properties and their proven antibacterial properties against a wide range of microorganisms (Oka, Tomioka, Tomita, Mishino, & Veda, 1994; Oloffs et al., 1994).

Nano-silver can be modified for better efficiency in diverse medicine and life sciences applications such as drug manufacturing advancement, protein detection and gene delivery (Geddes et al., 2003; Mahmoudi, Simchi, Imani, Milani, & Stroeve, 2008). The copper metal fabrication of miniaturised nano-devices that integrate electronic, photonic, chemical and biological features is important for future electronic and sensing devices (Sashiwa & Aiba, 2004). Surface plasmon band (SPB) sensors are widely used for biosensing, especially as affinity biosensors (Kadir, Patrick, & Geddes, 2006). The intrinsic properties of metal nanoparticles are mainly governed by their sizes, shape, composition, crystallinity, and structure. The requirement for LSPR (localised surface plasmon resonance) is a large negative real and a small imaginary dielectric function. A number of metals (i.e. Li, Na, Al, In, Ga, and Cu) meet this criterion and in theory should support plasmon resonances for at least part of the UV–Vis–NIR region (Bohren & Huffman, 1983; Zeman & Schatz, 1987). However, most of these metals are either unstable, or prone to surface oxidation that can significantly affect their optical properties. As a result of surface oxidation, the plasmonic properties of copper nanoparticles (CuNPs) have not received much attention compared to silver plasmonic properties.

Polymer–metal nanoparticle composites research has received much attention in recent years due to an increased interest in their application in opto-electronics Korchev, Bozack, Slaten, and Mills (2004), nonlinear optical devices Inouye, Tanaka, Tanahashi, Hattori, and Nakatsuka (2000) and colour filters (Dirix, Bastiaansen, Caseri, & Smith, 1999). The size-dependent electronic and optical properties of the nanoparticles inbuilt with the optical transparency and mechanical stability of the polymer films signify their importance in many applications. Among the wide variety of polymer matrices, biopolymers are often the first choice as they are naturally available, cheaper as well as easy to synthesise and modify for various applications and more importantly, they are

* Corresponding author. Tel.: +27 011 559 6180; fax: +27 011 559 6425.
E-mail address: amishra@uj.ac.za (A.K. Mishra).

0144-8617/$ – see front matter © 2012 Elsevier Ltd. All rights reserved.
http://dx.doi.org/10.1016/j.carbpol.2012.10.008

environmentally friendly. Moreover, the availability of oxygen-rich functional groups of the biopolymers and their affinity towards metals make them an ideal matrix for the stabilisation of nanoparticles (Liu, He, Durham, Zhao, & Roberts, 2008). Biopolymers such as cellulose, starch and alginic acid have been previously used for the stabilisation of nanoparticles (Brayner, Vaulay, Fiévet, & Coradin, 2007; He, Kunitake, & Nakao, 2003; Raveendran, Fu, & Wallen, 2003). Chitosan, isolated from chitin, is the linear and partly acetylated (1–4)-2-amino-2-deoxy-<beta>-D-glucan (Muzzarelli, 1977, 2012), particularly well known for metal ion chelation (Muzzarelli, 2011) and for biological applications (Muzzarelli, 2009), as it is hydrophilic, biocompatible, biodegradable, non-antigenic and non-toxic (Muzzarelli, 2010).

In addition, chitosan is known to facilitate drug delivery across cellular barriers and transiently open the tight junctions between epithelial cells (Dodane, Khan, & Merwin, 1999). Few reports are available on synthesis of metal nanoparticles of smaller size in chemically modified chitosan matrices for various prominent applications (Bodnar, Hartmann, & Borbely, 2005; Ding, Xia, & Zhang, 2006; Sashiwa & Aiba, 2004). The green synthesis of gold nanoparticles has been used previously on the derivative of chitosan which has the functional group amine as reducing agent and thiocarbamide as stabiliser for the nanoparticles embedded in the film or as colloidal solution (Tiwari, Mishra, Mishra, Arotiba, & Mamba, 2011).

The objective of this study was to synthesise metal nanoparticles such as AgNPs and CuNPs in an aqueous solution. Chemically modified chitosan was used as a reducing and capping or stabilising agent for the metal nanoparticles. The morphology and stability of the metal nanoparticles were examined using transmission electron microscopy (TEM) and UV–Vis spectroscopy. The possible capping mechanism of the nanoparticle was monitored by the Fourier transform infra-red spectroscopy (FT-IR). Optical and spectroscopy properties such as SPB, fluorescence, photoluminescence and surface enhanced Raman scattering (SERS) of the nanoparticles were also studied.

2. Materials and methods

2.1. Materials

All compounds were of analytical grade and used as received. Acetic acid (99.7%), silver nitrate ($AgNO_3$) (99.9%) and copper dichloride ($CuCl_2{\cdot}2H_2O$) (99.0%) were purchased from Merck (South Africa) and thiocarbohydrazide (99.0% synthetic grade) was obtained from Sigma Aldrich (South Africa). Pyridine 2,6-dicarboxylic acid sourced from Merck (South Africa) was esterified using methanol to form pyridine 2,6-dimethylcarboxylate. Chitosan (75% deacetylated, low molecular weight) was purchased from Sigma–Aldrich (South Africa), and deionised (DI) water was used throughout the experiment.

2.2. Synthesis

2.2.1. Chitosan-N-2-methylidene-hydroxy-pyridine-6-methylidene-hydroxy-thiocarbohydrazide (CSPTH)

Modified chitosan (CSPTH) was synthesised, using a previously reported procedure (Tiwari, Mishra, Mishra, Arotiba, et al., 2011). The synthesis of CSPTH is summarised as follows: chitosan (3.0 g) was dissolved in 2% acetic acid (200 mL). A solution of pyridine-2,6 dimethylcarboxylate (12.5 g in 100 mL ethanol) was added to the chitosan solution and refluxed for 8 h. The mixture was kept overnight under ambient conditions. A gel was formed after neutralisation using 1 mM NaOH and this was completely precipitated in acetone. The filtered gel was dried in hot air (oven) at 60 °C for 3 h. The yield of the dried white solid product was 2.50 g (80%). The product was treated again with thiocarbohydrazide. The dried product (2.0 g) was dissolved in 4% acetic acid (100 mL) and 5.0 g thiocarbohydrazide in 2% acetic acid (200 mL). Both solutions were mixed and refluxed for 24 h. The product was neutralised using 1 mM NaOH and after this the gel formed was precipitated in acetone. The solid precipitate was dried in an oven at the 60 °C for 3 h. A brown yellowish solid product [1.25 g (75%)] was obtained. The structure of the produced modified chitosan derivative is shown in Fig. 1.

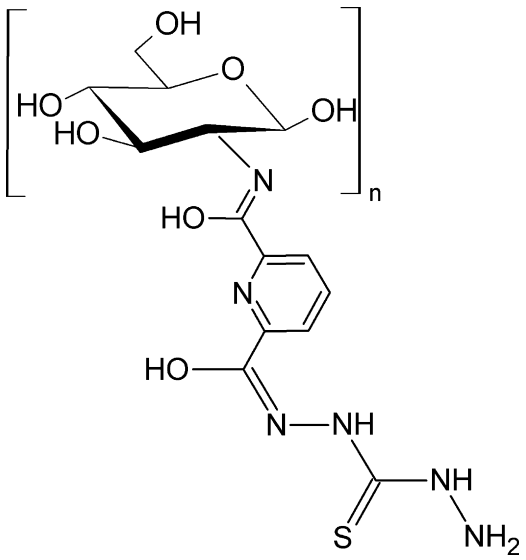

Fig. 1. Chemical structure of the chitosan-N-2-methylidene-hydroxy-pyridine-6-methylidene hydroxy thiocarbohydrazide (CSPTH).

2.2.2. Synthesis of silver and copper nanoparticles on the chemically modified chitosan biopolymer matrix (CSPTH-AgNPs/CuNPs)

Chemically modified chitosan (CSPTH) solutions (10 mg/mL) were prepared in 2% aqueous acetic acid w/v ratio. Silver nitrate and copper dichloride hydrate solutions (10 mM) were added to the modified chitosan biopolymer matrix (CSPTH) in 1:1 (v/v) ratio. The colloidal metal nanoparticle and modified chitosan biopolymer solution were heated at 60 °C for 2 h and then stirred for 1 h, after which the temperature was reduced to 30 °C. The acronyms CSPTH, CSPTH-AgNPs, and CSPTH-CuNPs were given to the modified chitosan biopolymers as stabilised silver and copper nanoparticles, respectively.

2.3. Characterisation

UV–Vis absorption spectroscopy measurements were performed on a Shimadzu UV-2450 PC dual-beam spectrophotometer using 1 cm path length quartz cuvettes. Spectra were collected for the aqueous solutions within the 200–800 nm spectral range. FTIR measurements of the biopolymer matrix with nanoparticles and their precursors were recorded on an FT-IR spectrophotometer (Perkin Elmer spectrum 100) equipped with a diamond/ZnSe universal ATR sampling accessory. Spectra were obtained in transmission mode over the 4000 cm^{-1} to 550 cm^{-1} wave-number region at a resolution of 4 cm^{-1} averaging 16 scans. The polymer film samples were prepared on glass slides and dried in the oven at 60 °C before being scraped off with a razor blade. Fluorescence spectroscopy was recorded on a Perkin Elmer LS 45 fluorescence spectrometer equipped with FL WinLab™ Software. An excitation

wavelength of 300 nm was applied to the aqueous solutions over the 200–900 nm wavelength range. Photoluminescence properties were observed at an excitation wavelength of 390 nm on a Perkin Elmer LS 45. Samples were analysed in aqueous solution over a wavelength range of 200–900 nm. Raman spectroscopic measurements were performed on a Perkin Elmer (RamanMicro 200) under ambient conditions.

Raman spectra were recorded on a Confocal Raman Microscope spectrometer equipped with a piezo scanner and a Nikon microscope. Signals were obtained on excitation of the samples by a laser (532 nm). Measurements were done with the objective beam path set at 50× (NA = 0.40) and an exposure time of 10 s. Spectra were recorded at 1 cm^{-1} resolution in the range 200–3200 cm^{-1} Raman shift. A Philips PANanalytical X'pert-PRO diffractometer system (40 kV, 40 mA) equipped with Cu Kα radiation source (λ = 0.1546 nm) and a curved graphite crystal was used to monitor diffraction patterns. A continuous scan rate of 1.06°/min was used to establish the energetically distinct sites for the crystallographic face of the metal nanoparticles. TEM measurements were performed on a Tecnai G^2 Spirit TEM instrument operating at 120 kV. Images were collected on a Gatan digital imaging system with the Power Mac 8600 computer Digital Micrograph software. Samples were prepared for TEM analysis by sonicating them for 10 min and then depositing small drops of the metal nanoparticle solutions (CSPTH-AgNPs and CuNPs) on the TEM lacy copper support grids for specimen suspension. The grids were allowed to dry before being mounted on the TEM sample holder.

3. Results and discussion

3.1. UV–Vis spectroscopy of the silver and copper nanoparticles (CSPTH-AgNPs/CuNPs) on the modified chitosan biopolymer

Small metal nanoparticles exhibit absorption of visible electromagnetic waves by the collective oscillation of conduction electrons at the surface. This is known as the surface plasmon resonance effect. The UV–Vis peak location may be influenced by the particle shape, size or multiple particle environments (Chandler-McLeod, McHenry, Beckman, & Roberts, 2003). Silver intermediate UV–Vis bands indicative of silver clusters composed of small numbers of atoms were observed. The peak observed at 270 nm is indicative of Ag_4^{2+} intermediates in agreement with literature (Petit, Lixon, & Pileni, 1993). The presence of plasmon absorption bands at 403 nm indicates the presence of silver nanoparticles within the colloidal solution of the modified chitosan biopolymer of silver nanoparticles (CSPTH-AgNPs). Metallic silver nanoparticles are commonly characterised by the absorption band located at 400 nm. This absorption band was observed at a wavelength between 380 nm and 420 nm depending on the size, shape, and surrounding environment of the silver nanoparticles (Fig. 2) (Petit et al., 1993).

In the case of the copper nanoparticles, the dipolar plasmon resonance was found to be dependent on the shape (triangular prisms, elongated particles, cylinders and spheres) of the nanoparticles. However, the lack of homogeneity in the size and shape of the samples and the lack of control over the inter-particle distances resulted in broadened surface plasmon resonances (Fig. 2), which suggest that the copper nanoparticles were not an ideal plasmonic material compared to silver nanoparticles (Ding et al., 2006). The silver nanoparticles showed improved plasmonic properties in the modified chitosan than the copper nanoparticles.

Two electronic wavelength bands at 247 nm and 358 nm were observed for the modified chitosan biopolymer (CSPTH) (Fig. 2). The CSPTH absorption bands at 257 nm (N—N chromophore) and 358 nm (C=N chromophore) disappeared or were largely shifted in

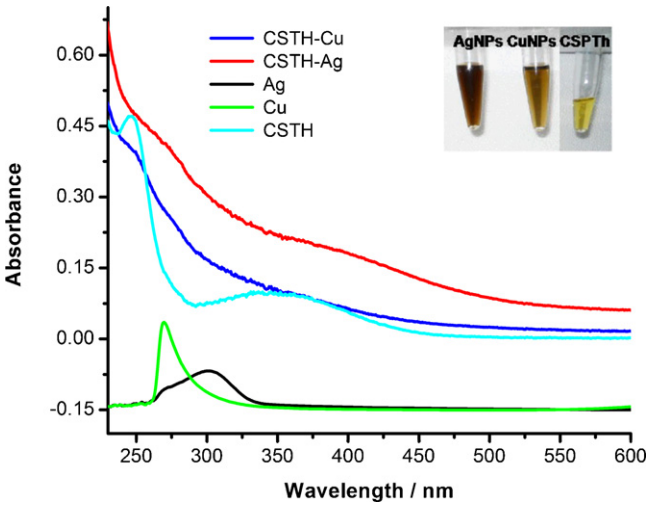

Fig. 2. UV–Vis absorption spectra indicating colloidal modified chitosan biopolymer silver nanoparticles (CSPTH-AgNPs), copper nanoparticles (CSPTH-CuNPs) and precursors CSPTH, $AgNO_3$ and $CuCl_2$ (10 mM) stock solution. Inserted picture indicates the colloidal solution of CSPTH, CSPTH-AgNPs/CuNPs.

the spectra of the nanoparticle modified chitosan colloidal aqueous solution (CSPTH-AgNPs/CuNPs) due to the possible transition between modified chitosan chromophore and metal nanoparticles through bonding as capping stabiliser (Tiwari, Mishra, Mishra, Mamba, et al., 2011).

3.2. Comparative FT-IR spectroscopy of the film of the modified chitosan biopolymer and silver and copper nanoparticle in chemically modified chitosan

To determine the interaction between the CSPTH and the metal nanoparticles, FT-IR spectra of CSPTH, CSPTH-AgNPs and CSPTH-CuNPs were compared (Fig. 3). Bonding between the metal nanoparticle and the thiocarbamide (—C=S) of CSPTH was expected due to electrostatic attraction between the metal nanoparticle and sulphur atom of the thiocarbamide (—C=S). Comparison of the spectra revealed that the IR band at 890 cm^{-1} corresponding to (—C=S) was absent or shifted to 930 cm^{-1} in the CSPTH-AgNPs and CSPTH-CuNPs spectra due to possible interaction between the

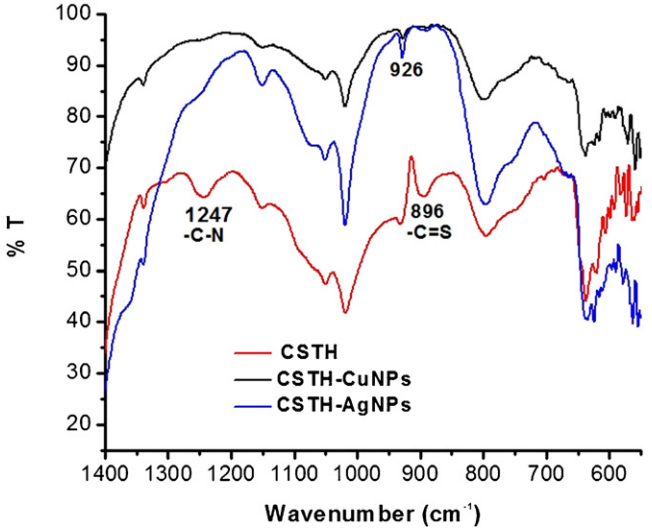

Fig. 3. Comparative FT-IR spectra for the chemically modified chitosan (CSPTH) and embedded metal nanoparticles on CSPTH (CSPTH-AgNPs and CSPTH-CuNPs).

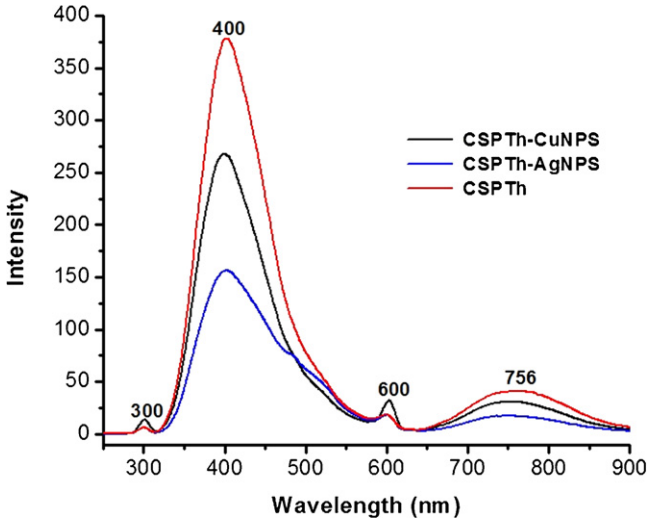

Fig. 4. Comparative fluorescence emission spectra of aqueous colloidal solution modified chitosan (CSPTH) and metal nanoparticles in CSPTH (CSPTH-AgNPs and CSPTH-CuNPs).

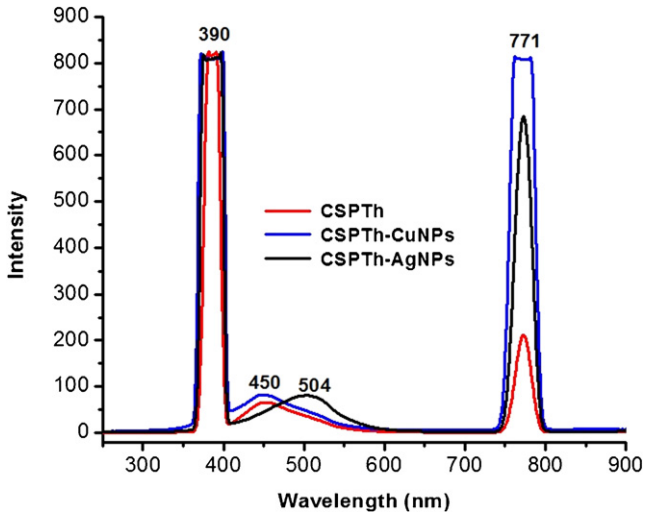

Fig. 5. Comparative photoluminescence spectra of the CSPTH, CSPTH-AgNPs and CSPTH-CuNPs colloidal solution.

metal nanoparticle and –(C=S). The IR band located at 1247 cm^{-1} was characteristic of the (—C—N) functionality of chitosan. This (—C—N) stretching band becomes flattened probably as a result of the bonding interaction between the metal nanoparticles and the (—C—N) group (Panigrahi et al., 2006; Tiwari, Mishra, Mishra, Arotiba, et al., 2011).

3.3. Fluorescence and photoluminescence spectroscopy of the silver and copper nanoparticles in the chemically modified chitosan biopolymer aqueous solution

Fluorescence enhancement may be attributed to the effect of the metal (Bharadwaj & Novotny, 2007; Lakowicz, 2006). As the metallic nanoparticles were irradiated with a UV light source, an enhanced electric field was created in the vicinity of the surface, the incident wavelength depending on the characteristics of the metallic nanoparticles. The field enhancement can affect the spontaneous decay rate and the photoluminescence intensity (Brolo et al., 2005). Fluorescence spectra of colloidal aqueous solution of modified chitosan biopolymer (CSPTH) and the colloidal aqueous solutions of CSPTH-AgNPs and CSPTH-CuNPs are shown in Fig. 4. A charge-transfer process was evidenced by a decrease in the fluorescence intensity. Silver and copper nanoparticle colloidal solutions as well as the modified chitosan biopolymer stock solutions (0.2 mL) were diluted to 2 mL using deionised water. On excitation of the solutions at 300 nm, quenching (decrease in the fluorescence intensity) was observed in the absorption and emission spectra of the metal nanoparticles (CSPTH-AgNPs and CSPTH-CuNPS). AgNPs exhibited more quenching than CuNPs at 400 nm and 756 nm. The secondary excitation peak was observed at 600 nm, double that of the excitation wavelength (300 nm) (Siwach & Sen, 2008; Wilcoxon, Martin, Parsapour, & Kelley, 1998).

The photoluminescence from the rough surface of the metal nanoparticles resulted from excitation of electrons from the occupied d-band into ground state level of the Fermi level (Fig. 5). Wilcoxon et al. (1998) proposed that a similar mechanism was responsible for nanocluster photoluminescence. The photoluminescence spectra were obtained for the colloidal nanoparticles by excitation at a wavelength of 390 nm. The secondary effect of double the excitation wavelength was observed at 780 nm with another peak at the 450 nm wavelength for CSPTH and CSPTH-CuNPs. However, for the CSPTH-AgNPs colloidal solution the maximum luminescence recorded was 504 nm.

The emission peak intensity for copper and silver nanoparticles was more enhanced than that of the modified chitosan biopolymer. Peaks at 450 nm and 504 nm were observed for CuNPs and AgNPs, respectively, due to their different electronic structure giving rise to emissions at different wavelengths even though the excitation was at the same wavelength. It was found that the CSPTH-CuNPs photoluminescence intensity was higher than that of the CSPTH-AgNPs secondary double excitation wavelength at 780 nm due to their distinctive absorption and excitation properties.

3.4. Raman spectroscopy in respect of the surface-enhanced Raman scattering (SERS) of the silver and copper nanoparticles on the chemically modified chitosan

Metal nanostructures have proven to be effective SERS-active substrates. According to the electromagnetic theory of SERS, enhancements depend on the excitation of the localised surface plasmon resonance, which is influenced by several significant parameters such as size, shape and the nature of the nanomaterial aggregates. Raman scattering was recorded for the colloidal solutions of the nanoparticles and modified chitosan (CSPTH-AgNPs, CuNPs-CSPTH and CSPTH) (Fig. 6). It was found that CSPTH-CuNPs had enhanced G (1382 cm^{-1}) and D (1851 cm^{-1}) band intensities compared to CSPTH, with the CSPTH-AgNPs showing the lowest intensities. The synthesised colloidal copper nanoparticles with chemically modified chitosan provided a better substrate for SERS and the study of compositional dependence of chemical adsorption and reactions on the surface of copper nanoparticles (Morones et al., 2005).

3.5. Powder X-ray diffraction (PXRD) studies of the silver and copper nanoparticles on the modified chitosan biopolymer colloidal matrix

The structures of the stabilised nanoparticle on the CSPTH were analysed by powder X-ray diffraction (PXRD). Fig. 7 shows the comparative XRD patterns of the CSPTH, CSPTH-CuNPs and CSPTH-AgNPs nanoparticles. It was observed that the characteristic sharp symmetric peak for the silver nanoparticle appeared at 2θ angles of 17.1°, 26.8° and 52.4° corresponding to the (1 0 1), (1 1 2) and (3 1 2) crystal planes, respectively. The patterns were similar to

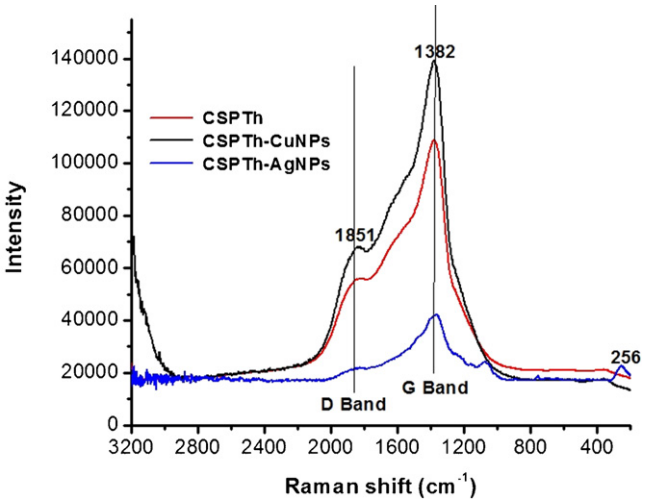

Fig. 6. Raman spectroscopy for the film of chemically modified chitosan (CSPTH) and stabilised silver and copper nanoparticles (CSPTH-AgNPs and CSPTH-CuNPs).

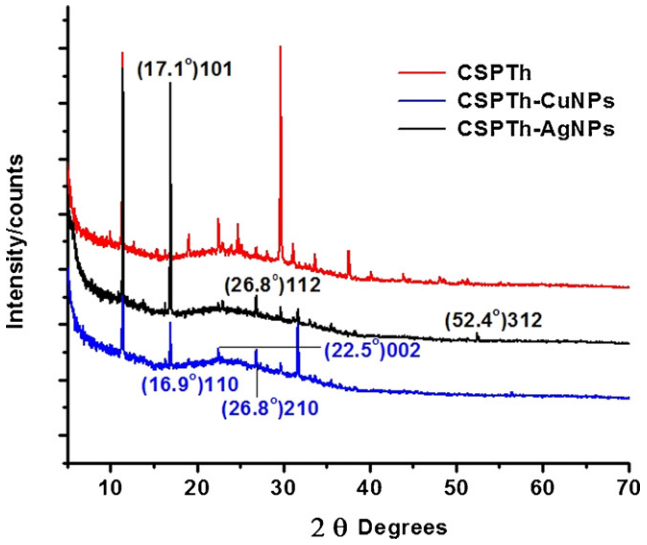

Fig. 7. PXRD pattern for the film of the chemically modified chitosan (CSPTH) and stabilised silver and copper nanoparticles (CSPTH-AgNPs and CSPTH-CuNPs).

the database of silver indium sulphide ($AgInS_2$) (pdf card number 04-007-4436). Copper nanoparticles (CSPTH-CuNPs) exhibited sharp peaks which were observed at angles of 16.9°, 22.5° and 26.8° which correspond to the (1 1 0), (2 1 0) and (0 0 2) crystal faces, respectively (pdf card number 00-023-0478). Each crystallographic face contains energetically distinct sites based on the atom density (Hatchett & White, 1996). The CSPTH-AgNPs peaks of the spectrum were found to have higher intensities/counts than the CSPTH-CuNPs. This may be due to the smaller size of the AgNPs compared to the CuNPs.

3.6. Transmission electron microscopy (TEM) studies

Transmission electron microscopy (TEM) observations of the colloidal solution of the metal nanoparticle for the CSPTH-AgNPs showed that the particles had an average diameter of less than 20 nm (Fig. 8a). All four images were taken over a period of one month (15 days after synthesis and 30 days after synthesis) from different sites of the sample with different resolutions, with the aim of establishing the stability of nanoparticles in the colloidal solution of the modified chitosan biopolymer in terms of the time factor. All nanoparticles were found to be well-dispersed in the modified chitosan colloidal solution. TEM analysis was also performed on the copper nanoparticles colloidal solution (CSPTH-CuNPs) to determine the particle distribution and size in the colloidal solution. The average diameter of the copper nanoparticles (CuNPs) was found to be less than 50 nm (Fig. 8b). TEM characterisation led to the conclusion that the modified chitosan biopolymer was a good stabiliser for copper and silver nanoparticles because the entire nanoparticles were found to be well-dispersed as individual units in the chemically modified chitosan colloidal solution. The modified chitosan biopolymer was a better stabiliser for the silver nanoparticles because silver nanoparticles were smaller in size than the copper nanoparticles. Similar results were observed by Panigrahi et al. (2006).

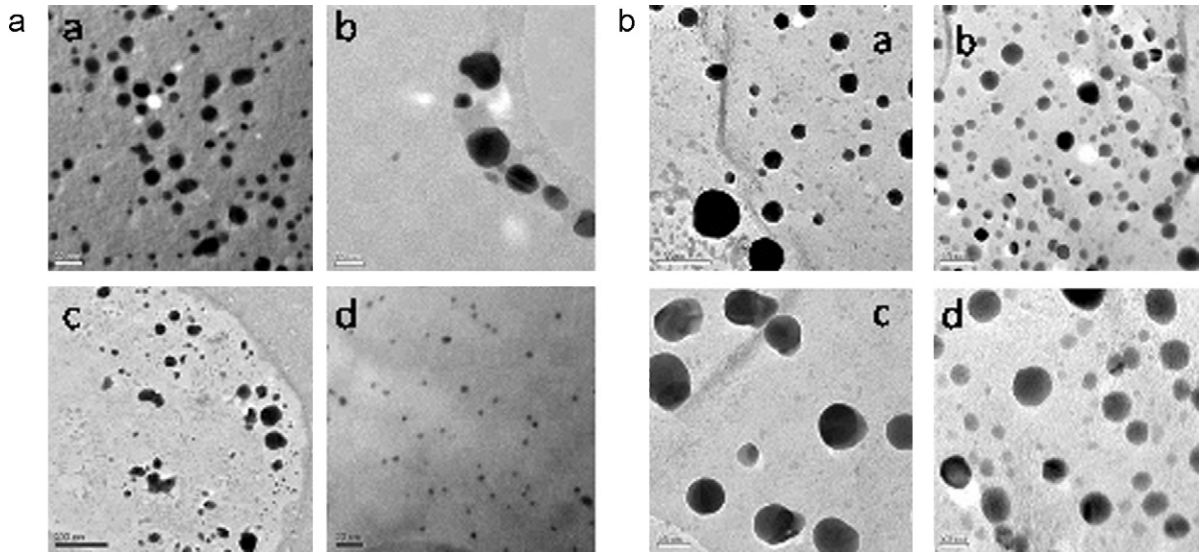

Fig. 8. (a) TEM images of the silver nanoparticle stabilised in the chemically modified chitosan (CSPTH-AgNPs) from the different region and resolution; (a) and (b) images taken 15 d after synthesis, and (c) and (d) images taken 30 d after synthesis. (b) TEM images of the copper nanoparticle stabilised on the chemically modified chitosan (CSPTH-CuNPs) from the different region and resolution; (a) and (b) images taken 15 d after synthesis, and (c) and (d) images taken 30 d after synthesis.

4. Conclusion

Chemically modified chitosan functionalised metal nanoparticles such as CuNPs and AgNPs were synthesised in an aqueous medium. The metal nanoparticles stabilised on modified chitosan biopolymer (CSPTH) were found to be stable for more than a month as revealed by TEM analysis, performed after one month of synthesis. The silver nanoparticles were found to be smaller in size (average size less than 20 nm) compared to the copper nanoparticles (average size of less than 50 nm). In the context of size and SPB, the modified chitosan was found to be a suitable stabiliser for the silver nanoparticles than for the copper nanoparticles. The FT-IR and UV–Vis spectra gave an indication of the capping of the nanoparticles with sulphur and oxygen. The SPB of silver nanoparticles was prominent compared to the SPB of copper nanoparticles. However, in terms of fluorescence, photoluminescence and Raman scattering, the intrinsic properties of the copper nanoparticles were found to be superior to those of the silver nanoparticles. The entire study showed that the synthesised copper and silver nanoparticles were stabilised in the aqueous medium (chemically modified chitosan biopolymer support) and can be used for various biocompatible applications in different scientific disciplines.

Acknowledgements

The authors acknowledge the University of Johannesburg (UJ) and UJ Commonwealth Fellowship for financial support for AD Tiwari. The authors are also grateful to Prof. Alexander Ziegler of the University of the Witwatersrand, Johannesburg, for TEM analyses.

References

Bharadwaj, P., & Novotny, L. (2007). Spectral dependence of single molecule fluorescence enhancement. *Optics Express*, *15*, 14266–14274.

Bodnar, M., Hartmann, J. F., & Borbely, J. (2005). Preparation and characterization of chitosan-based nanoparticles. *Biomacromolecules*, *6*, 2521–2527.

Bohren, C. F., & Huffman, D. R. (1983). *Absorption and scattering of light by small particle*. New York: John Wiley & Sons.

Brayner, R., Vaulay, M. J., Fiévet, F., & Coradin, T. (2007). Alginate-mediated growth of Co, Ni, and CoNi nanoparticles: Influence of the biopolymer structure. *Chemistry of Materials*, *19*, 1190–1198.

Brolo, A. G., Kwok, S. C., Moffitt, M. G., Gordon, R., Riordon, J., & Kavanagh, K. L. (2005). Enhanced fluorescence from arrays of nanoholes in a gold film. *Journal of American Chemical Society*, *127*, 14936–14941.

Chandler-McLeod, M., McHenry, R. S., Beckman, E. J., & Roberts, C. B. (2003). Synthesis and stabilization of silver metallic nanoparticles and premetallic intermediates in perfluoropolyether/CO_2 reverse micelle systems. *Journal of Physical Chemistry B*, *107*, 2693–2700.

Cobley, C. M., Rycenga, M., Zhou, F., Li, Z. Y., & Xia, Y. (2009). Controlled etching as a route to high quality silver nanospheres for optical studies. *Journal of Physical Chemistry C*, *113*, 16975–16982.

Ding, Y., Xia, X., & Zhang, C. (2006). Synthesis of metallic nanoparticles protected with *N*,*N*,*N*-trimethyl chitosan chloride via a relatively weak affinity. *Nanotechnology*, *17*, 4156–4162.

Dirix, Y., Bastiaansen, C., Caseri, W., & Smith, P. (1999). Oriented pearl-necklace arrays of metallic nanoparticles in polymers: A new route toward polarization-dependent color filters. *Advanced Materials*, *11*, 223–277.

Dodane, V., Khan, M. A., & Merwin, J. R. (1999). Effect of chitosan on epithelial permeability and structure. *International Journal of Pharmaceutics*, *182*, 21–32.

Geddes, C. D., Cao, H., Gryczynski, I., Gryczynski, Z., Fang, J., & Lakowicz, R. J. (2003). Metal-enhanced fluorescence (MEF) due to silver colloids on a planar surface: Potential applications of indocyanine green to *in vivo* imaging. *Journal of Physical Chemistry A*, *107*, 3443–3449.

Hatchett, D. W., & White, H. S. (1996). Electrochemistry of sulfur adlayers on the low-index faces of silver. *Journal of Physical Chemistry*, *100*, 9854–9859.

He, J., Kunitake, T., & Nakao, A. (2003). Facile *in situ* synthesis of noble metal nanoparticles in porous cellulose fibers. *Chemistry of Materials*, *15*, 4401–4406.

Inouye, H., Tanaka, K., Tanahashi, I., Hattori, T., & Nakatsuka, H. (2000). Ultrafast optical switching in a silver nanoparticle system. *Japanese Journal of Applied Physics*, *39*, 5132–5133.

Kadir, A., Patrick, H., & Geddes, C. D. (2006). Metal-enhanced fluorescence from silver nanoparticle-deposited polycarbonate substrates. *Journal of Materials Chemistry*, *16*, 2846–2852.

Korchev, A. S., Bozack, M. J., Slaten, B. L., & Mills, G. (2004). Polymer-initiated photogeneration of silver nanoparticles in SPEEK/PVA films: Direct metal photopatterning. *Journal of American Chemical Society*, *126*, 10–11.

Lakowicz, J. R. (2006). *Principles of fluorescence spectroscopy* (p. 841).(3rd ed.). Baltimore, USA: Springer.

Li, W., Camargo, P. H. C., Lu, X., & Xia, Y. (2009). Dimers of silver nanospheres: Facile synthesis and their use as hot spots for surface-enhanced Raman scattering. *Nano Letters*, *9*, 485–490.

Liu, J. C., He, F., Durham, E., Zhao, D., & Roberts, C. B. (2008). Polysugar-stabilized Pd nanoparticles exhibiting high catalytic activities for hydro dechlorination of environmentally deleterious trichloroethylene. *Langmuir*, *24*, 328–336.

Mahmoudi, M., Simchi, A., Imani, M., Milani, S. A., & Stroeve, P. (2008). Optimal design and characterization of superparamagnetic iron oxide nanoparticles coated with polyvinyl alcohol for targeted delivery and imaging. *Journal of Physical Chemistry B*, *112*, 14470–14481.

Morones, J. R., Elechiguerra, J. L., Camacho, A., Holt, K., Kouri, J. B., & Ramirez, J. T. (2005). The bactericidal effect of silver nanoparticles. *Nanotechnology*, *16*, 2346–2353.

Muzzarelli, R. A. A. (1977). *Chitin*. Oxford, UK: Pergamon Press.

Muzzarelli, R. A. A. (2009). Chitins and chitosans for the repair of wounded skin, nerve, cartilage and bone. *Carbohydrate Polymers*, *76*, 167–182.

Muzzarelli, R. A. A. (2010). Chitins and chitosans as immunoadjuvants and non-allergenic drug carriers. *Marine Drugs*, *8*(2), 292–312.

Muzzarelli, R. A. A. (2011). Potential of chitin/chitosan-bearing materials for uranium recovery: An interdisciplinary review. *Carbohydrate Polymers*, *84*, 54–63.

Muzzarelli, R. A. A. (2012). Nanochitins and nanochitosans, paving the way to eco-friendly and energy-saving exploitation of marine resources. In K. Matyjaszewski, & M. Möller (Eds.), *Polymer science: A comprehensive reference* (pp. 153–164). Amsterdam: Elsevier BV.

Oka, M., Tomioka, T., Tomita, K., Mishino, A., & Veda, S. (1994). Inactivation of enveloped viruses by a silver-thiosulfate complex. *Metal Based Drugs*, *1*, 511.

Oloffs, A., Crosse-Siestrup, C., Bisson, S., Rinck, M., Rudoluh, R., & Gross, U. (1994). Biocompatibility of silver-coated polyurethane catheters and silver coated Dacron material. *Biomaterial*, *15*, 753–758.

Panigrahi, S., Praharaj, S., Basu, S., Ghosh, S. K., Jana, S., Pande, S., et al. (2006). Self-assembly of silver nanoparticles: Synthesis, stabilization, optical properties, and application in surface-enhanced Raman scattering. *Journal of Physical Chemistry B*, *110*, 13436–13444.

Petit, C., Lixon, P., & Pileni, M. P. (1993). *In situ* synthesis of silver nanocluster in AOT reverse micelles. *Journal of Physical Chemistry*, *97*, 12974–12983.

Quiros, I., Yamada, M., Kubo, K., Mizutani, J., Kurihara, M., & Nishihara, H. (2002). Preparation of alkanethiolate-protected palladium nanoparticles and their size dependence on synthetic conditions. *Langmuir*, *18*, 1413–1418.

Raveendran, P., Fu, J., & Wallen, S. L. (2003). Completely green synthesis and stabilization of metal nanoparticles. *Journal of American Chemical Society*, *125*, 13940–13941.

Sashiwa, H., & Aiba, S. (2004). Chemically modified chitin and chitosan as biomaterials. *Progress in Polymer Science*, *29*, 887–908.

Sharma, J., Chhabra, R., Cheng, A., Brownell, J., Liu, Y., & Yan, H. (2009). Control of self-assembly of DNA tubules through integration of gold nanoparticles. *Science*, *323*, 112–116.

Siwach, O. P., & Sen, P. (2008). Synthesis and study of fluorescence properties of Cu nanoparticles. *Journal of Nanoparticle Research*, *10*, 107–114.

Sun, Y., & Xia, Y. (2002). Shape-controlled synthesis of gold and silver nanoparticles. *Science*, *298*, 2176–2179.

Tiwari, A. D., Mishra, A. K., Mishra, S. B., Arotiba, O. A., & Mamba, B. B. (2011). Green synthesis and stabilization of gold nanoparticles in chemically modified chitosan matrices. *International Journal of Biological Macromolecules*, *48*, 682–687.

Tiwari, A. D., Mishra, A. K., Mishra, S. B., Mamba, B. B., Maji, B., & Bhattacharya, S. (2011). Synthesis and DNA binding studies of Ni(II), Co(II), Cu(II) and Zn(II) metal complexes of N^1,N^5-bis[pyridine-2-methylene]-thiocarbohydrazone Schiff-base ligand. *Spectrochimica Acta Part A: Molecular and Biomolecular Spectroscopy*, *79*, 1050–1056.

Wilcoxon, J. P., Martin, J. E., Parsapour, F., & Kelley, D. F. (1998). Photoluminescence from nanosize gold clusters. *Journal of Chemical Physics*, *108*, 9137–9143.

Yavuz, M. S., Cheng, Y., Chen, J., Cobley, C. M., Zhang, Q., Rycenga, M., et al. (2009). Gold nanocages covered by smart polymers for controlled release with near-infrared light. *Nature Materials*, *8*, 935–939.

Zeman, E. J., & Schatz, G. C. (1987). An accurate electromagnetic theory study of surface enhancement factors for silver, gold, copper, lithium, sodium, aluminum, gallium, indium, zinc and cadmium. *Journal of Physical Chemistry*, *91*, 634–643.